

Dynamic modes of $k\pi$ skyrmions excited by spin waves

Ruiyu Huang(黄瑞玉), Chunjun Qi(祁纯军), Zhe Yi(易哲), Wei Liu(刘巍), Lin Chen(陈琳), and Zhikuo Tao(陶志阔)
Citation: Chin. Phys. B, 2026, 35 (**7**): 077508. DOI: 10.1088/1674-1056/ae118e
http://cpb.iphy.ac.cn; http://iopscience.iop.org/cpb

What follows is a list of articles you may be interested in

Engineering nonreciprocal damping and polarization of spin waves in ferromagnetic domain wall via Dzyaloshinskii-Moriya interaction and spin-transfer torque

Xiang Liu(刘想), Xiguang Wang(王希光), Zhixiong Li(李志雄), Xiufeng Han(韩秀峰), and Guanghua Guo(郭光华)
Chin. Phys. B, 2026, 35 (**4**): 047502. DOI: 10.1088/1674-1056/ae2771

Analogous Faraday effect of spin waves propagating in ferromagnetic nanotubes

Li Zhou(周利), Zhixuan Ren(任芷萱), and Ming Yan(颜明)
Chin. Phys. B, 2026, 35 (**4**): 047501. DOI: 10.1088/1674-1056/ae1ff7

Directly tunable magnon frequency comb effect based on domain wall

Xiaoxue Yang(杨霄雪), Huiting Li(李慧婷), Xue-Feng Zhang(张雪枫), Xiao-Ping Ma(马晓萍), Je-Ho Shim(沈帝虎), Yingjiu Jin(金迎九), and Hong-Guang Piao(朴红光)
Chin. Phys. B, 2025, 34 (**10**): 107507. DOI: 10.1088/1674-1056/ade856

Magnon behavior in YIG film under microwave excitation investigated by Brillouin light scattering

Guofu Xu(徐国服), Kang An(安康), Wenjun Ma(马文俊), Xiling Li(李喜玲), C. K. Ong, Chi Zhang(张驰), and Guozhi Chai(柴国志)
Chin. Phys. B, 2025, 34 (**6**): 067507. DOI: 10.1088/1674-1056/add24c

Orbital magnetic field effect on spin waves in a triangular lattice tetrahedral antiferromagnetic insulator

Pi-Ye Zhou(周丕烨), Xiao-Hui Li(李晓慧), and Yuan Wan(万源)
Chin. Phys. B, 2025, 34 (**6**): 067501. DOI: 10.1088/1674-1056/adca1f

---

Dynamic modes of $k\pi$ skyrmions excited by spin waves

Ruiyu Huang(黄瑞玉), Chunjun Qi(祁纯军), Zhe Yi(易哲), Wei Liu(刘巍), Lin Chen(陈琳), and Zhikuo Tao(陶志阔)†

College of Electronic and Optical Engineering & College of Flexible Electronics, Nanjing University of Posts and Telecommunications, Nanjing 210003, *China*

(Received 26 July 2025; revised manuscript received 28 September 2025; accepted manuscript online 10 October 2025)

The dynamic modes of the $k\pi$ skyrmions excited by spin waves are investigated. Firstly, formations of $k\pi$ skyrmions are investigated. Secondly, breathing modes of $k\pi$ skyrmions excited by spin waves are studied, and it is found that spin waves can effectively excite breathing modes. The breathing frequencies excited by spin waves are identical to the intrinsic frequencies for 1π skyrmions, while the breathing frequencies excited by spin waves are larger than the intrinsic frequencies for 2π skyrmions and 3π skyrmions. Thirdly, gyration modes of $k\pi$ skyrmions excited by spin waves are studied, and it is found that spin waves can effectively excite gyration modes. In particular, the ranges of the trajectories driven by spin waves with intrinsic gyration frequencies are larger than the ranges of the trajectories driven by spin waves with other frequencies. This work promotes the understanding of $k\pi$ skyrmion dynamics under spin-wave excitation and provides a platform for developing spin-wave-based microwave devices utilizing $k\pi$ skyrmions.

Keywords: $k\pi$ skyrmions, spin waves, dynamic properties

PACS: 75.30.Ds, 75.80.+q, 85.70.Ay, 12.39.Dc

DOI: 10.1088/1674-1056/ae118e **CSTR:** 32038.14.CPB.ae118e

1. Introduction

Recent advances in spintronics have introduced novel topological magnetic textures such as magnetic vortices[1] and skyrmions[2,3] as information carriers. Skyrmions, in particular, have emerged as a focus of intense research. Compared to traditional domain walls, skyrmions have gained prominence due to their non-trivial topologies, sub-nanometer dimensions, and low critical current density. As topological magnetic structures, skyrmions can be stabilized through competing interactions including exchange interaction, Zeeman energy, and Dzyaloshinskii–Moriya interaction (DMI).[4,5] Since the prediction of skyrmion existence in magnetic films and multilayers by Bogdanov and Rößler in 2001,[6] experimental breakthroughs have followed; Mühlbauer's team first observed skyrmions in MnSi crystals through neutron scattering in 2009.[7] Beyond conventional skyrmions, $k\pi$ skyrmions have drawn attention for their unique magnetization profiles. These rotationally symmetric vortex-like solitons,[8] also termed $k\pi$ radial vortices, exhibit $(k+1)\pi$ magnetization rotation from core to boundary. Unlike conventional skyrmions ($k = 1$), their spatial profiles ($k > 1$) feature additional out-of-plane domains.[9–11] Among these, of particular interest are the topological charge properties of the $k\pi$ skyrmion: $|Q| = 1$ for odd k and $Q = 0$ for even k. Particularly, this duality enables unique applications, for example, the 2π skyrmion ($Q = 0$) can circumvent skyrmion Hall effect constraints while achieving higher mobility than conventional skyrmions,[21] offering solutions for nanoscale motion control challenges.

Furthermore, spin waves can propagate in magnetically ordered materials and cannot dissipate Joule heating, which is an obstacle in the semiconductor-based electronics. Then, subsequent studies revealed spin wave modes in skyrmion lattices via numerical simulations,[12] while materials like Cu_2OSeO_3 demonstrated characteristic resonance modes — breathing mode (excited by out-of-plane magnetic fields) and gyration modes (activated by in-plane magnetic fields),[13–19] which correlated with skyrmion structures shaped by material parameters and external static fields.[20–23] Meanwhile, reported works reveal regulation mechanisms for $k\pi$ skyrmion stability via perpendicular fields, DMI, and mechanical strain.[24–29] As fundamental excitations in magnetic systems, spin waves may influence $k\pi$ skyrmion configurations and dynamics through energy or momentum transfer mechanisms. However, few systematic investigations of the dynamic characteristics of $k\pi$ skyrmions excited by spin waves are reported. In this work, the dynamic modes of the $k\pi$ skyrmions excited by spin waves are investigated theoretically. Firstly, the numerical simulation method is presented. Next, formations of $k\pi$ skyrmions are investigated. Then, the breathing modes and gyration modes of $k\pi$ skyrmions excited by spin waves are investigated.

2. Model and method

The numerical simulations are performed using the Object–Oriented MicroMagnetic Framework (OOMMF) public code. To obtain dynamic responses of skyrmions, the Landau–Lifshitz–Gilbert (LLG) equation is numerically

†Corresponding author. E-mail: zktao@njupt.edu.cn

© 2026 Chinese Physical Society and IOP Publishing Ltd. All rights, including for text and data mining, AI training, and similar technologies, are reserved.

solved

$$\frac{\partial m(r,t)}{\partial t} = -\mu_0\gamma(m(r,t)\times H_{\text{eff}}) + \alpha\left(m(r,t)\times\frac{\partial m(r,t))}{\partial t}\right), \quad (1)$$

where μ_0 is the vacuum permeability, γ the gyromagnetic ratio, α the damping parameter, and $m(r,t)$ the normalized magnetization.[30,31] The effective field H_{eff} can be calculated by

$$H_{\text{eff}} = -\frac{1}{\mu_0 M_{\text{s}}}\frac{\partial E_{\text{tot}}}{\partial m(r,t)}, \quad (2)$$

where H_{eff} includes contributions from the exchange field (H_{ex}), perpendicular magnetic anisotropy field (H_{PMA}), Zeeman field (H_{Ze}), demagnetization field (H_{demag}), DMI field (H_{DMI}), and E_{tot} is the total free energy encompassing all interactions. In magnetic systems, the magnetization vector aligns with the total effective field direction due to energy competition, resulting in zero torque along the magnetization direction. Minimizing E_{tot} numerically yields static configurations, while dynamic responses are analyzed by applying alternating microwave fields to modify the Zeeman term.

In this work, cobalt-based cylindrical ferromagnetic thin films are employed to hold $k\pi$ skyrmions. For simulations, the film is discretized into 2 nm×2 nm×2 nm cells. The parameters used are: a static magnetic field $H_Z = 1\times10^5$ A/m, exchange stiffness $A_{\text{ex}} = 1.5\times10^{-11}$ J/m, gyromagnetic ratio $\gamma = 2.211\times10^5$ m/(A·s), and saturation magnetization $M_{\text{s}} = 5.8\times10^5$ A/m. The DMI constant D and perpendicular anisotropy constant K are set to specific combinations to generate $k\pi$ skyrmions with distinct topological numbers (k).

3. Results and discussion

3.1. The formations of $k\pi$ skyrmions

Firstly, Néel-type $k\pi$ skyrmions with $k = 1$, 2, and 3 are realized in cobalt-based cylindrical ferromagnetic thin films with a diameter of 200 nm and a thickness of 2 nm, as shown in Fig. 1(a). For $k\pi$ skyrmions, the magnetization undergoes multiple rotations between the magnetic core and collinear regions, where k represents the number of sign reversals in the out-of-plane magnetization component m_z along the radial direction. Here, the numerically calculated Q values are −0.882, 0.018, and −0.836 for $k = 1$, 2, and 3, respectively, which are consistent with the analytical values ($Q = -1$ for $k = 1$, 3 and $Q = 0$ for $k = 2$). The magnetization m_z along the x-axis for 1π, 2π, and 3π skyrmions is shown in Fig. 1(b). It can be seen that the magnetizations preserve radial symmetry, and the count of magnetization rotation increases as the topological number (k) increases. In addition, the morphological manipulations can be seen in Fig. S1 in the supplementary materials.

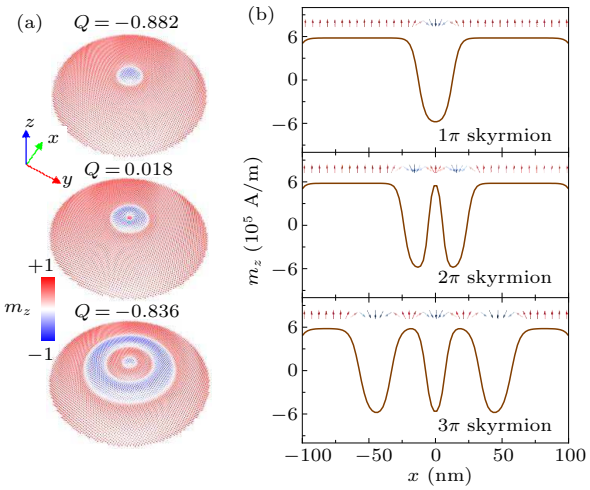


Fig. 1. (a) The $k\pi$ skyrmions on a cylindrical ferromagnetic thin film. ($D = 3.2$ mJ/m^2 and $K = 0.6\times10^6$ J/m^3 for the 1π skyrmion, $D = 3.95$ mJ/m^2 and $K = 0.8\times10^6$ J/m^3 for the 2π skyrmion, $D = 3.185$ mJ/m^2 and $K = 0.5\times10^6$ J/m^3 for the 3π skyrmion). (b) The out-of-plane magnetization m_z of 1π skyrmion, 2π skyrmion, and 3π skyrmion along x-axis.

3.2. Breathing modes excited by spin waves

Secondly, breathing modes of $k\pi$ skyrmions excited by spin waves are investigated. We adopt the cobalt-based rectangular ferromagnetic thin film shown in Fig. 2(a) as the simulation platform, with the dimensions of 1000 nm×1000 nm×2 nm. In order to identify the intrinsic frequency of the breathing mode, a sinc-function magnetic field $\boldsymbol{H}_z(t) = H_{z0}\text{sinc}(\omega_{\text{H}}(t-t_0))\cdot\hat{z}$ ($H_{z0} = 200$ A/m, $\omega_{\text{H}} = 2\pi f$ with $f = 100$ GHz, $t_0 = 0.1$ ns) is applied to the whole x–y plane for 3 ns. The evolution of the average m_z over the entire region (m_z–t relations) can be collected and the power spectra from the fast Fourier transform (FFT) of m_z–t relations can be calculated, from which we can get the intrinsic frequency of the breathing mode. Here, parameters of $D = 3.2$ mJ/m^2 and $K = 0.6\times10^6$ J/m^3, $D = 3.95$ mJ/m^2 and $K = 0.8\times10^6$ J/m^3, $D = 3.185$ mJ/m^2 and $K = 0.5\times10^6$ J/m^3 are chosen to hold the 1π skyrmion, the 2π skyrmion, and the 3π skyrmion, respectively.

As shown in Fig. 2(b), only one FFT peak can be observed for the 1π skyrmion which corresponds to the intrinsic breathing mode. Particularly, the breathing modes shift to the higher frequencies with decreasing the D values. For the 2π skyrmion as shown in Fig. 2(c), two intrinsic breathing modes f_{21} and f_{22} can be obtained. In addition, the breathing modes f_{21} almost do not move with changing the D values, while the breathing modes f_{22} shift to the higher frequencies with decreasing the D values, which is similar to that for 1π skyrmion. Especially, up to three breathing modes can be obtained in the 3π skyrmion as shown in Fig. 2(d). Similar to that for the 1π skyrmion and the 2π skyrmion, the breathing modes f_{31} almost do not move while the breathing modes f_{33} shift to the higher frequencies with decreasing the D values. Typically, the breathing modes f_{32} can be obtained by choosing parame-

ters precisely, and would be annihilated with increasing the D values.

To further investigate the characteristics of resonant mode, spatial profiles of the magnetization fluctuations $\delta m_z(t)$ are presented in Figs. 2(e)–2(j). The $k\pi$ skyrmions are driven under a *sin*-magnetic field $\boldsymbol{H}'_z(t) = H'_{z0}\sin(\omega_{\rm H}t)\cdot\hat{\boldsymbol{z}}$ with $H'_{z0} =$ 200 A/m and $\omega_{\rm H} = 2\pi f$ with $f = 9.33$ GHz for the 1π skyrmion, 4.67 GHz and 32.33 GHz for the 2π skyrmion, 0.67 GHz, 12 GHZ, and 16 GHz for the 3π skyrmion. Several snapshots of the spatial profiles of the magnetization $m_z(t)$ from 1.5 ns to 2.3 ns are saved when the dynamic resonances hold stable. Then, magnetic variation $\delta m_z(t) = m_z(t) - m_z(0)$ can be achieved, which describes the spatial profiles of the resonant fluctuation. The static profile $m_z(0)$ is also shown in Figs. 2(e)–2(j). It can be seen that the magnetization fluctuations perform strong intensity around the regions of the $k\pi$ skyrmions with $m_z(0) = 0$ and preserve radial symmetry, which indicates the breathing mode. At the same time, it can be seen that the magnetization fluctuations show different profiles with varied topological numbers (k).

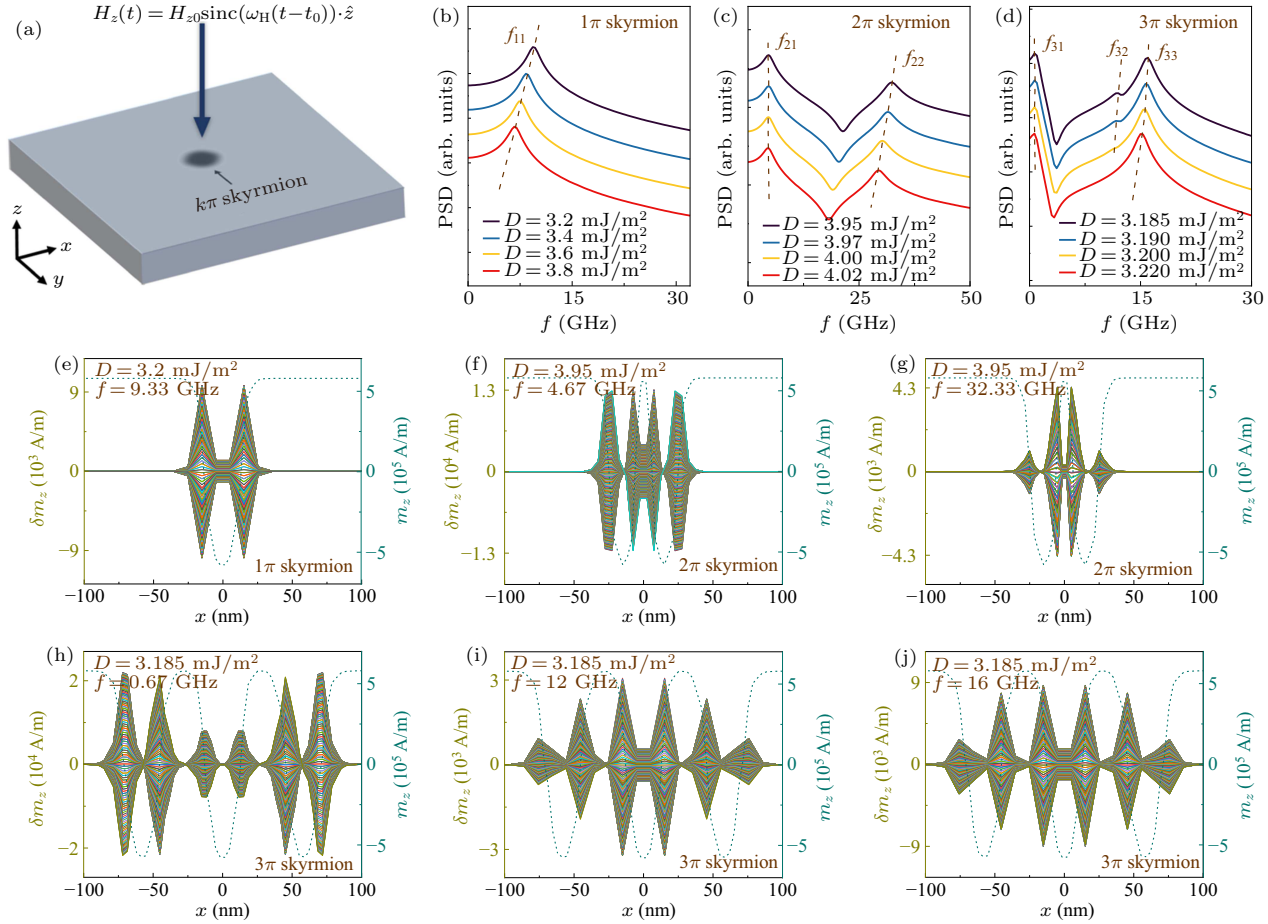


Fig. 2. (a) Schematic diagram of identifying the breathing mode of $k\pi$ skyrmions with applying an out-of-plane magnetic field along the z-axis to the whole ferromagnetic thin film. FFT power spectrum of m_z–t relations under for (b) 1π skyrmion, (c) 2π skyrmion, and (d) 3π skyrmion. Spatial profiles of the breathing mode with (e) 1π skyrmion, (f)–(g) 2π skyrmion, and (h)–(j) 3π skyrmion.

Furthermore, the dynamic properties of breathing modes excited by spin waves are investigated. As shown in Fig. 3(a), we apply a sinusoidal magnetic field $\boldsymbol{H}_{\rm sw}(t) = H_{\rm sw0}\sin(\omega_{\rm H}t)\cdot\hat{x}$ ($H_{\rm sw0} = 200$ A/m, $\omega_{\rm H} = 2\pi f$ with $f = 100$ GHz) to the left rectangular area of the film to excite spin waves. Then, the spin waves will propagate toward the $k\pi$ skyrmions located at the film center and interact with the $k\pi$ skyrmions, as shown in Fig. 3(b). Therefore, the spin waves stimulate the breathing modes of the $k\pi$ skyrmions in the center of the cobalt-based rectangular ferromagnetic thin film. Similar to the process of investigating the intrinsic breathing modes by applying alternating magnetic fields to the whole ferromagnetic thin film, the evolutions of the average m_z over the entire region are collected and the corresponding FFT are calculated, from which we can get the frequencies of the breathing modes excited by spin waves.

Figures 3(c), 3(d), and 3(e) present the frequencies of breathing modes excited by spin waves for the 1π skyrmion, the 2π skyrmion, and the 3π skyrmion, respectively. As shown in Figs. 3(c), 3(d), and 3(e), one breathing mode, two breathing modes and three breathing modes can be observed for the 1π skyrmion, the 2π skyrmion, and the 3π skyrmion, respectively. Meanwhile, f_{11}, f_{22}, and f_{33} shift to higher frequencies with decreasing D values, while f_{21} and f_{31} do not move. Especially, the breathing modes f_{32} present extremely weak intensities.

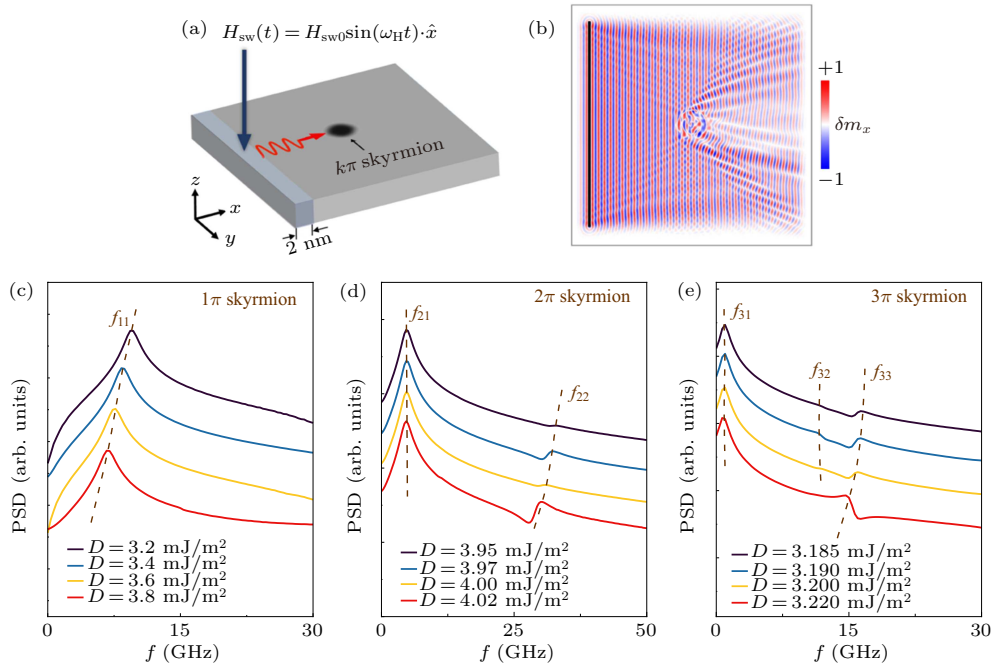


Fig. 3. (a) Schematic diagram of identifying the breathing mode of $k\pi$ skyrmions excited by spin waves. (b) Illustration of magnetic film subjected to a microwave source applied in a rectangular region (black bar). FFT power spectrum of m_z–t relations for (c) 1π skyrmion, (d) 2π skyrmion, and (e) 3π skyrmion.

Table 1. Difference of breathing frequencies between intrinsic excitation and spin-wave excitation.

	1π skyrmion	2π skyrmion		3π skyrmion		
	f_{11}	f_{21}	f_{22}	f_{31}	f_{32}	f_{33}
D_1	0	0	0.34	0.33	–	0.67
D_2	0	0	1.00	0.33	–	0.66
D_3	0	0	0.67	0.33	–	0.67
D_4	0	0	0.67	0.33	–	0.33

To compare the intrinsic breathing frequencies with the breathing frequencies excited by spin waves, we summarize the values of frequency difference Δf ($\Delta f = f_{\text{spin waves}} - f_{\text{intrinsic}}$) in Table 1. It can be seen that the breathing frequencies excited by spin waves are identical to the intrinsic frequencies for 1π skyrmions with different D values. For 2π skyrmions, the breathing frequencies f_{21} are identical, but the breathing frequencies f_{22} excited by spin waves are a little larger than the intrinsic frequencies with different D values. For 3π skyrmions, the peaks related to f_{32} are broad and weak, so we have not compared the differences. Similar to 2π skyrmions, the breathing frequencies f_{31} and f_{31} excited by spin waves are larger than the intrinsic frequencies with different D values. Especially, the differences for 3π skyrmions are obviously larger than those for 2π skyrmions; the reason for this is still under investigation. However, it is proved that spin waves can effectively excite breathing modes of $k\pi$ skyrmions.

3.3. Gyration modes excited by spin waves

Thirdly, gyration modes of $k\pi$ skyrmions excited by spin waves were investigated. For the conventional 1π skyrmion, the gyration modes include counterclockwise (CCW) gyration mode and clockwise (CW) gyration mode, which can be excited and observed when an alternating magnetic field is applied in parallel to the skyrmion surface.[21–23] In this section, following the methodology of the previous section, parameters of $D = 3.2$ mJ/m^2 and $K = 0.6 \times 10^6$ J/m^3, $D = 3.95$ mJ/m^2 and $K = 0.8 \times 10^6$ J/m^3, $D = 3.185$ mJ/m^2 and $K = 0.5 \times 10^6$ J/m^3 are chosen to realize the 1π skyrmion, the 2π skyrmion, and the 3π skyrmion, respectively.

As shown in Fig. 4(a), in order to get the intrinsic gyration modes, we apply an in-plane sinc-function magnetic field $\boldsymbol{H}_x(t) = H_{x0}\text{sinc}(\omega_H(t - t_0)) \cdot \hat{x}$ with $H_{x0} = 200$ A/m, $\omega_H = 2\pi f$ ($f = 100$ GHz), $t_0 = 1$ ns, and t ranging from 0 to 10 ns to the whole film. Figure 4(d) shows the corresponding FFT power spectrum of the m_x–t relationships for 1π skyrmion. It can be seen that a prominent resonance peak was observed at 32.6 GHz, which corresponds to the intrinsic gyration mode. To further demonstrate the characteristics of this gyration mode, the trajectory of the guiding center under a sinusoidal driving field $\boldsymbol{H}'_x(t) = H'_{x0}\sin(\omega_H t) \cdot \hat{x}$ with $H'_{x0} = 200$ A/m, $\omega_H = 2\pi f_{\text{driving}}$ ($f_{\text{driving}} = 32.6$ GHz) is presented in Fig. 4(e). The coordinates (R_x, R_y) of the guiding

center are defined as follows:[32–34]

$$R_x = \frac{\iint xq\mathrm{d}x\mathrm{d}y}{\iint q\mathrm{d}x\mathrm{d}y}, \quad R_y = \frac{\iint yq\mathrm{d}x\mathrm{d}y}{\iint q\mathrm{d}x\mathrm{d}y}, \tag{3}$$

where q is the topological charge density. It is obvious that the guiding center presents a CCW circular trajectory, which indicates a dynamic gyration mode. Especially, the topological number Q can be 0 for 2π skyrmion, and it is not suitable to use Eq. (3) to calculate the coordinates of the guiding center for 2π skyrmion. Therefore, we only discuss the gyration modes of 1π and 3π skyrmions excited by spin waves.

Next, the dynamic properties of gyration modes excited by spin waves are investigated. As shown in Fig. 4(c), a sinusoidal magnetic field $\boldsymbol{H}_{\mathrm{sw}}(t) = H_{\mathrm{sw0}}\sin(\omega_{\mathrm{H}}t)\cdot\hat{x}$ is applied to the left rectangular area of the film to excite spin waves, which is same to that of the investigation on the breathing modes excited by spin waves. As shown in Figs. 4(f)–4(j), the guiding centers present a linear trajectory driven by spin wave with frequency of 32.6 GHz, and elliptical trajectories driven by spin waves with frequency of 10 GHz, 20 GHz, 30 GHz, and 40 GHz.

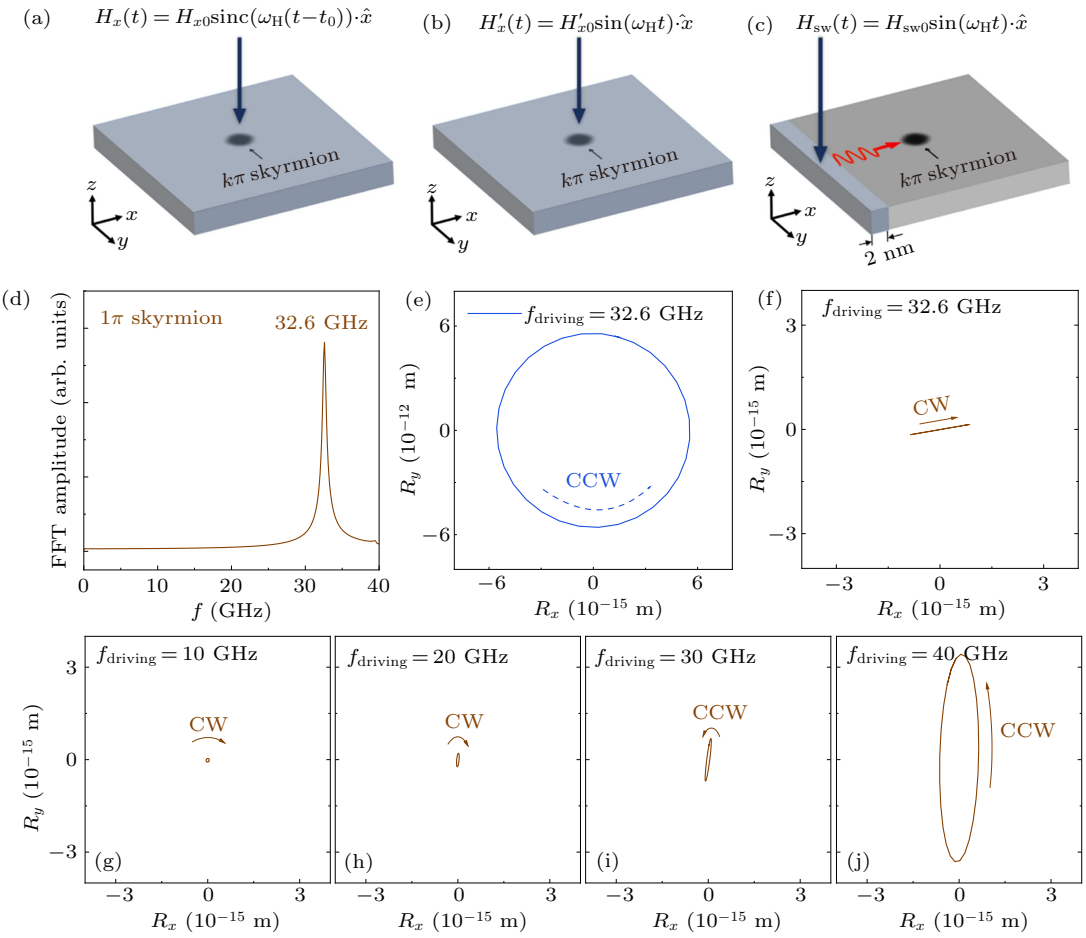


Fig. 4. (a) Schematic diagram of identifying the gyration modes of $k\pi$ skyrmions with applying an in-plane sinc-magnetic field along the x-axis to the whole ferromagnetic thin film. (b) Schematic diagram of demonstrating the gyration motion driven under an in-plane sin-magnetic field. (c) Schematic diagram of identifying the gyration mode of $k\pi$ skyrmions excited by spin waves. (d) FFT power spectrum of m_x–t relations of the 1π skyrmion with applying an in-plane sinc-magnetic field. (e) The trajectory of the guiding center (R_x, R_y) under sin-magnetic field driving at 32.6 GHz. The trajectories of the guiding center (R_x, R_y) excited by spin waves with driving frequency of (f) 32.6 GHz, (g) 10 GHz, (h) 20 GHz, (i) 30 GHz, and (j) 40 GHz.

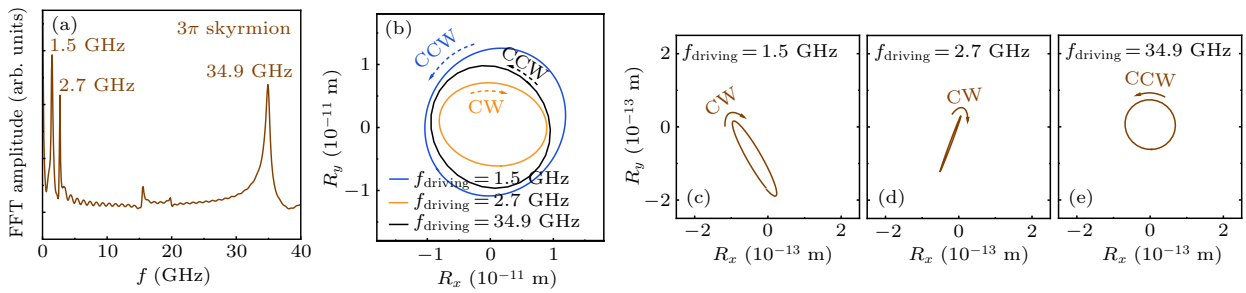


Fig. 5. (a) FFT power spectrum of m_x–t relations of the 3π skyrmion with applying an in-plane sinc-magnetic field. (b) The trajectories of the guiding center (R_x, R_y) under sin-magnetic field driving at intrinsic gyration frequencies. (c)–(e) The trajectories of the guiding center (R_x, R_y) excited by spin waves with driving frequency of 1.5 GHz, 2.7 GHz, and 34.9 GHz for 3π skyrmions.

Furthermore, 3π skyrmions excited by spin waves are investigated. Figure 5(a) displays the FFT power spectrum of the 3π skyrmion, where gyration resonance peaks appear at 1.5 GHz, 2.7 GHz, and 34.9 GHz, indicating its multi-mode dynamic response. Figure 5(b) shows the trajectories of the guiding center (R_x, R_y) under *sin*-magnetic field driving at intrinsic gyration. It can be seen that the gyration modes present two CCW and one CW motions. Figures 5(c)–5(e) show the trajectories of the guiding center (R_x, R_y) under spin wave driving at intrinsic gyration. It can be seen that the gyration modes present one CCW and two CW motions. It is suggested that the guiding centers driven by spin waves with different frequencies all present elliptical trajectories. Particularly, the ranges of the trajectories driven by spin waves with intrinsic gyration frequencies are larger than the ranges of the trajectories driven by spin waves with other frequencies. The trajectories with driving frequencies of 10 GHz∼40 GHz can be seen in Figs. S3(a)–S3(d) in supplementary materials.

4. Conclusion

In summary, the dynamic modes of the $k\pi$ skyrmions excited by spin waves are investigated. Firstly, formations of $k\pi$ skyrmions are investigated by varying the DMI constant D and perpendicular anisotropy constant K. Next, the breathing modes and gyration modes of $k\pi$ skyrmions excited by spin waves are investigated. It is proved that spin waves can effectively excite breathing modes of $k\pi$ skyrmions. The values of frequency differences are summarized to compare the intrinsic breathing frequencies with the breathing frequencies excited by spin waves. The breathing frequencies excited by spin waves are identical to the intrinsic frequencies for 1π skyrmions, while the breathing frequencies excited by spin waves are larger than the intrinsic frequencies for 2π skyrmions and 3π skyrmions. Meanwhile, spin waves can effectively excite gyration modes of $k\pi$ skyrmions. The guiding centers driven by spin waves with different frequencies all present elliptical trajectories. More importantly, the ranges of the trajectories driven by spin waves with intrinsic gyration frequencies are obviously larger than the ranges of the trajectories driven by spin waves with other frequencies. This work enhances the understanding of $k\pi$ skyrmion dynamics under spin-wave excitation and provides a platform for developing spin-wave-based microwave devices utilizing $k\pi$ skyrmions.

References

[1] Shinjo T, Okuno T, Hassdorf R, Shigeto K and Ono T 2000 *Science* **289** 930
[2] Sampaio J, Cros V, Rohart S, Thiaville A and Fert A 2013 *Nat. Nanotechnol.* **8** 839
[3] Yu X Z, Kanazawa N, Onose Y, Kimoto K, Zhang W Z, Ishiwata S, Matsui Y and Tokura Y 2011 *Nat. Mater.* **10** 106
[4] Dzyaloshinsky I 1958 *J. Phys. Chem. Solids* **4** 241
[5] Moriya T 1960 *Phys. Rev. Lett.* **4** 228
[6] Bogdanov A N and Rößler U K 2001 *Phys. Rev. Lett.* **87** 037203
[7] Mühlbauer S, Binz B, Jonietz F, Pfleiderer C, Rosch A, Neubauer A, Georgii R and Boöni P 2009 *Science* **323** 915
[8] Jiang J, Wu Y, Kong L, Wang Y, Li J, Xiong Y and Tang J 2021 *Acta Mater.* **215** 117084
[9] Binasch G, Grünberg P, Saurenbach F and Zinn W 1989 *Phys. Rev. B* **39** 4828
[10] Baibich M N, Broto J M, Fert A, Nguyen V D F and Petroff F 1988 *Phys. Rev. Lett.* **61** 2472
[11] Vigo-Cotrina H and Guzman-Arana A 2023 *J. Magn. Magn. Mater.* **585** 171122
[12] Mochizuki M 2012 *Phys. Rev. Lett.* **108** 017601
[13] Onose Y, Okamura Y, Seki S, Ishiwata S and Tokura Y 2012 *Phys. Rev. Lett.* **109** 037603
[14] Kim J V, Garcia-Sanchez F, Sampaio J, Moreau-Luchaire C, Cros V and Fert A 2014 *Phys. Rev. B* **90** 064410
[15] McKeever B F, Rodrigues D R, Pinna D, Abanov A, Sinova J and Everschor-Sitte K 2019 *Phys. Rev. B* **99** 054430
[16] Garanin D A, Jaafar R and Chudnovsky E M 2020 *Phys. Rev. B* **101** 014418
[17] Wang W, Beg M, Zhang B, Kuch W and Fangohr H 2015 *Phys. Rev. B* **92** 020403
[18] Moon K W, Kim D H, Je S G, Chun B S, Kim W, Qiu Z Q, Choe S B and Hwang C 2016 *Sci. Rep.* **6** 20360
[19] Jin C, Song C, Wang J, Xia H, Wang J and Liu Q 2017 *J. Appl. Phys.* **122** 223901
[20] Liu Y, Yin G, Zang J, Shi J and Lake R K 2015 *Appl. Phys. Lett.* **107** 152411
[21] Lonsky M and Hoffmann A 2020 *Phys. Rev. B* **102** 104403
[22] Liu Y, Lake R K and Zang J 2018 *J. Magn. Magn. Mater.* **455** 9
[23] Miriyala V P K, Zhu Z, Liang G and Fong X 2019 *J. Magn. Magn. Mater.* **486** 165271
[24] Song C, Ma Y, Jin C, Wang J, Xia H, Wang J and Liu Q 2019 *New J. Phys.* **21** 083006
[25] Liu X, Zhu Q, Zhang S, Liu Q and Wang J 2015 *AIP Adv.* **5** 087137
[26] Mehmood N, Song X, Tian G, Hou Z, Chen D, Fan Z, Qin M, Gao X and Liu J M 2019 *J. Phys. D: Appl. Phys.* **53** 014007
[27] Zhang Y, Shi M, Wang W, Xu X, Tian M, Song D and Du H 2023 *Nano Lett.* **23** 10205
[28] Vigo-Cotrina H, Monteiro D, Urruchua J and Guimarães A 2022 *J. Magn. Magn. Mater.* **560** 169665
[29] Zhao R, Hu C, Ji L, Chen W and Zhang X 2020 *Sci. China-Phys. Mech. Astron.* **63** 267511
[30] Jonietz F, Mühlbauer S, Pfleiderer C, Neubauer A, Münzer W, Bauer A, Adams T, Georgii R, Böni P, Duine R A, Everschor K, Garst M and Rosch A 2010 *Science* **330** 1648
[31] Yu X Z, Kanazawa N, Zhang W Z, Nagai T, Hara T, Kimoto K, Matsui Y, Onose Y and Tokura Y 2012 *Nat. Commun.* **3** 988
[32] Papanicolaou N and Tomaras T N 1991 *Nucl. Phys. B* **360** 425
[33] Dai Y Y, Wang H, Tao P, Yang T, Ren W J and Zhang Z D 2013 *Phys. Rev. B* **88** 054403
[34] Yu D, Sui C, Schulz D, Berakdar J and Jia C 2021 *Phys. Rev. Appl.* **16** 034032